Received 13 May 2022; accepted 29 June 2022. Date of publication 4 August 2022; date of current version 29 August 2022.

Digital Object Identifier 10.1109/OJAP.2022.3192115

Wideband Corrugated Feedhorns, for Radar, Communications, Radiometry and Quasi-Optics

DANIEL J. SUNG, NINA THOMSEN, STUART MACPHERSON, ROBERT I. HUNTER, SAMIUR RAHMAN (Member, IEEE), DUNCAN A. ROBERTSON (Member, IEEE), RICHARD J. WYLDE, AND GRAHAM M. SMITH

School of Physics and Astronomy, University of St Andrews, St Andrews KY169SS, U.K.

CORRESPONDING AUTHOR: G. M. SMITH (e-mail: gms@st-andrews.ac.uk)

This work was supported in part by Engineering and Physical Sciences Research Council, U.K., under Grant EP/R013705/1, and in part by IAA Funding.

ABSTRACT A wide variety of desirable antenna beam patterns can be synthesized by optimal excitation and phasing of the HE_{11} and HE_{12} modes in scalar corrugated feedhorns. However, the bandwidth of such two-mode horns is often limited by modal dispersion. In this paper we introduce a class of low dispersion, two-mode feedhorns that can operate, in some cases, over operating bandwidths of 40-50%. We provide example designs that include horns with high coupling efficiency to: 1) a pure HE_{11} mode for single-mode excitation of corrugated pipe transmission lines; 2) a LG_{00} and LG_{02} combination for radiometry, with narrow beams; 3) a pure Laguerre Gaussian LG_{00} mode for quasi-optical instrumentation with constant phase centers; 4) a constant gain antenna for uniform illumination with frequency; 5) Airy patterns or "top hat" patterns for radar or communications applications, designed to maximize aperture efficiencies when used with larger reflect or lens antennas. More generally, we show methods to generate and phase multiple HE_{1n} modes, to synthesize symmetric output beams at any desired frequency or gain.

INDEX TERMS Aperture antennas, antenna feeds, corrugated horns, horn antennas, quasi-optics, ultra-wideband antennas.

I. INTRODUCTION

CORRUGATED feedhorns have long been the gold standard for feed antennas that require the highest levels of beam quality combined with the lowest levels of cross-polarization. They find numerous applications in quasi-optical instrumentation, in communication systems, astronomical telescopes, imaging radar and radiometry for remote sensing.

Corrugated feedhorns are essentially a series of mode transformers. The standard design usually involves transforming from an input rectangular TE_{10} waveguide mode to a circular TE_{11} mode and then to a dominant HE_{11} mode at the horn throat. The horn profile then determines the amplitude of higher order modes excited within the horn and their relative phasing at the aperture that in turn determine the final radiation beam pattern.

Today, beam patterns from corrugated feedhorns can be modelled with extraordinary accuracy using mode matching software and there is now a significant literature on their design and optimization including a number of books and review articles [1]–[4]. Often, initial designs are based on general geometric arguments and improved by computational optimization programs [5]. This has encouraged a view that corrugated feedhorn design is largely a solved problem. However, practical experience has shown this is simply not true, especially over wide bandwidths. Due to the very large parameter space it is nearly always necessary to start from a near optimal solution, strongly informed by previous designs, and guided by the intuition of the design engineer [5]. There are always trade-offs in performance, and it is rarely clear from first principles if published designs are close to optimal.

This work is licensed under a Creative Commons Attribution 4.0 License. For more information, see https://creativecommons.org/licenses/by/4.0/

This paper aims to establish optimal mode sets for common applications, and provide example designs that excite these mode sets, with low dispersion, over wide bandwidths.

The waveguide modes in corrugated feedhorns are most conveniently expressed as a set of HE_{1n} and EH_{1n} modes but have often been (less helpfully) expressed as set of TE_{1n} and TM_{1n} modes in the literature, as it is usually these modes that are directly calculated in mode matching software

All advanced corrugated feedhorn designs involve excitation of higher order modes within the feedhorn and a number of wideband designs have been described in the literature. Teniente has described a wideband design based on two stacked Gaussian profiles with < -30 dB sidelobes over 40% bandwidths [6]. Dual profile designs covering 20% and 30% bandwidths have been described for the LFI [7] and HFI [8] of the Planck telescope. These horns are part of a wider family of Gaussian profiled horns whose bandwidth is discussed in [9]. Other wideband designs covering 50% bandwidths, mainly targeting aperture efficiency, have also been described for the ALMA telescope [10].

However, virtually no papers tackle the design problem from the point of view of first identifying the optimal HE_{1n} mode set optimal for a given application. We are also not aware of any that then explicitly try to minimize modal dispersion to maximize bandwidth for a specific desired excitation. This is the design approach we have taken here, where we believe we demonstrate significantly improved wideband performance relative to previous designs in the literature.

In most practical cases, the mode conversion process in a corrugated horn is dominated by the HE_{11} mode converting to higher order HE_{1n} or EH_{1n} modes. The coupling Λ_{1n} of the HE_{11} mode to a different HE_{1n} mode, at any point in the horn, is proportional to the slope of the profile dr/dL divided by the profile cross-section radius r where L is the longitudinal distance along the horn axis [11], given by:

$$\Lambda_{1n} \propto \frac{dr/dL}{r} \tag{1}$$

with different constants of proportionality for different modes (lower for higher order modes). Thus, higher order modes will always be excited within a corrugated horn for any non-trivial profile. In this paper the normalized amplitude of a HE_{1n} mode, at a given radius r, is specified as a_{1n} where $\Sigma {a_{1n}}^2 \sim 1$ (neglecting the usually very small contribution from EH modes). The relative phase of the HE_{1n} mode with respect to the HE_{11} mode is specified as θ_{1n}. At any given point an excited HE_{1n} mode can interfere constructively or destructively with an existing propagating HE_{1n} mode, depending on their relative phases. Thus, it is possible to design profiles where certain modes interfere destructively and cancel at the aperture, while favorable modes are enhanced. It is also possible to bring any two given modes into phase at the aperture by simply adding a straight parallel length of corrugated guide, where no extra higher order mode excitation takes place.

In a traditional long conical corrugated horn with a constant slope profile, a small amount of HE_{12} mode will always be excited and end up approximately 90° out of phase with the HE_{11} mode at the aperture. It is the relative phasing of this extra mode that accounts for both the curved phase front at the aperture and the position of the phase center inside the horn. For compact horns with wide flare angles, this phasing can also lead to a degradation in the output beam profile with respect to a pure HE_{11} mode design. For this particular case, methods to reduce HE_{12} excitation can improve beam quality, as previously described by Clarricoats *et al.* [2] and Olver and Xiang [12].

As an alternative, it is possible to add a parallel section to a conical horn (or other profiles) that adds another 270° of relative phase shift to bring the two modes back into phase at the aperture. If the amplitude of the HE_{12} mode is chosen correctly this can significantly improve the quality of the beam. This is the design principle behind the $\sin^2$-parallel horn we have described before [13], which is now used in many quasi-optical systems. This horn is relatively easy to design, and typically produces highly symmetric beams with -37 dB to -40 dB sidelobes at the center frequency (limited by unwanted excitation of the HE_{13} mode). This is, in effect, a variation on the well-known smooth walled Potter horn design, and works well over 20% bandwidths, limited by modal dispersion.

We have also described a more compact version of this design with a tanh-linear profile that optimized the mode amplitudes for both the HE_{12} and HE_{13} modes (0.31 and 0.03 respectively) [14]. We tested a 20 dBi horn using this design, which had >99.95% coupling to a fundamental Gaussian beam with sidelobes at the -60 dB level at 94 GHz, and sidelobes close to -40 dB over a 16% bandwidth [15]. Now although the bandwidth and performance of this type of horn is significantly better than a Potter horn, the effective bandwidth is nevertheless still limited by modal dispersion, which causes beam distortion and movement of phase centers at the band edges.

The design challenge for wideband horns is thus to excite an HE_{12} mode with a target amplitude a_{12} and relatively constant phase θ_{12} (usually $|\theta_{12}| < 35°$) over a wide frequency range, whilst reducing excitation of all other unwanted higher modes, usually the EH_{11} and HE_{13} modes.

In this paper, we propose a set of dual-profiled horn designs that have very low modal dispersion and hence can operate over 40-50% fractional bandwidths.

In many of these two-section horns the first section excites a pure HE_{11} mode over a wide frequency range at the approximate desired aperture radius r_0. The second section of the horn then excites the required higher order modes and brings them into phase (or out of phase) with the HE_{11} mode at the aperture.

Section II first identifies the optimal HE_{1n} mode excitations for common applications and shows that it is often sufficient just to excite and correctly phase the HE_{12} mode with respect to the HE_{11} mode. Section III examines how the

HE_{12} mode content defines the effective phase center and beam waist, and thus the gain of the horn, as well as discussing other important metrics of horn performance such as compactness, return loss and cross-polar performance. Section IV then provides a number of illustrative wideband designs for a variety of applications.

All data shown in this paper are based on horn simulations using the mode matching software CORRUG (S.M.T. Consultancies Ltd.),[1] which derives the full scattering matrix at each corrugation. Simulations of co-polar and cross-polar beam patterns from this package have been experimentally validated many times by multiple international groups over a wide range of frequencies. For example, projects which feature CORRUG designed feedhorns include: the HFI Planck space telescope, which operates in 8 bands from 100 GHz to 800 GHz [8]; a limb sounder at 600 GHz for the International Space Station [16]; and more recently in the design of the quad-band TROPICS pathfinder cubesat system [17]. We have previously used CORRUG to design feedhorns with sidelobes as low as −60 dB [15]. In each case excellent agreement was found with measured antenna patterns. It should be noted that full wave simulation packages such as HFSS or CST Microwave Studio are less suited to optimizing corrugated feed designs, as they take considerably longer to simulate beam patterns accurately, especially for some of the relatively high gain (∼25 dBi) horns used to illustrate performance in this paper.

II. OPTIMAL HE_{1N} MODE SETS

For many wideband applications it is sufficient to consider excitation of just the HE_{11} and HE_{12} modes, and only exceptionally the HE_{13} mode. In all applications considered here, the HE_{12} mode should ideally be in phase ($\theta_{12} = 0°$), or out of phase ($\theta_{12} = 180°$), at the aperture. The amplitude a_{12} of the HE_{12} excitation is chosen dependent on the application. Fig. 1 shows the effect on the aperture mode pattern of exciting just the HE_{11} mode and HE_{12} modes for four different HE_{12} amplitudes: $a_{12} = 0$, $a_{12} = +0.31$, $a_{12} = -0.37$ and $a_{12} = +0.81$ where a plus sign indicates the two modes are in phase and a minus sign indicates they are 180° out of phase at the aperture.

Fig. 2 then shows the resulting expected far field beam patterns. These respectively produce, the typical beam pattern obtained from a HE_{11} mode, a good approximation to a fundamental Gaussian mode, a "top hat" pattern and an Airy pattern. Note the Airy and "top hat" patterns are effectively Fourier transform pairs. These beam patterns are of interest when the aperture efficiency of a system is the primary design goal.

A. PURE HE_{11} HORN

Excitation of a pure HE_{11} mode (i.e., $a_{11} = 1$, $a_{1n} = 0$ for $n > 1$) is useful whenever the design goal is to transmit power over relatively long distances, with very low loss, using a corrugated pipe. Corrugated pipe transmission lines are commonly used in fusion plasma heating and diagnostics, high power mm-wave radar systems, high frequency electron magnetic resonance and dynamic nuclear polarization experiments. If other higher order HE_{1n} modes are excited within the pipe these modes will continuously move in and out of phase with the HE_{11} mode, making the output beam pattern a function of frequency and pipe length. Pure HE_{11} mode horns and pipes are also potentially useful in horn-to-horn, quasi-optical, materials characterization measurements using VNAs. In these systems it is important to avoid higher order modes being trapped resonantly inside the system and to have a constant phase center at the horn aperture.

A feed of radius r_0 that produces a pure HE_{11} mode will couple with 98% efficiency to a fundamental Laguerre Gaussian LG_{00} mode with a beam waist radius of 0.6435

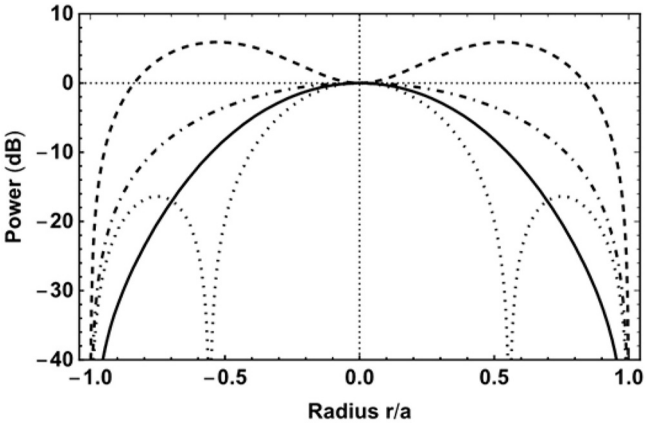

FIGURE 1. Power patterns at the feedhorn aperture for various HE_{12} mode content and phases: $a_{12} = -0.37$ (dashed line corresponding to a high aperture efficiency "top hat" feedhorn), $a_{12} = 0$ (dot-dashed line corresponding to pure HE_{11} mode), $a_{12} = +0.31$ (solid line corresponding to feed with high Gaussicity), $a_{12} = +0.81$ (dotted line corresponding to feed with high coupling efficiency to the main and first sidelobe of an Airy beam).

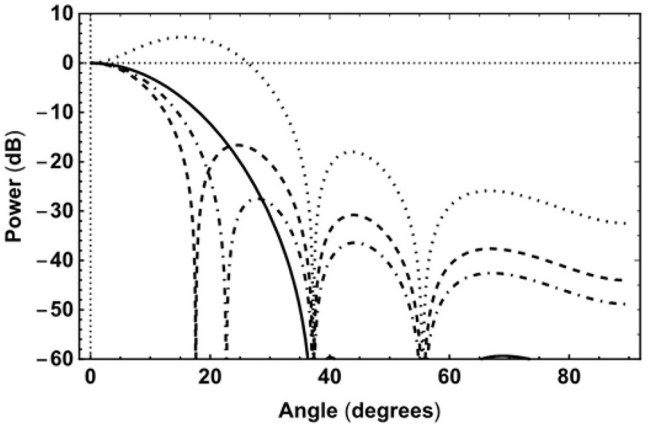

FIGURE 2. Normalized far field power patterns for the various HE_{12} mode amplitudes and phases of Fig. 1 with: $a_{12} = -0.37$ (dashed line corresponding to a high aperture efficiency feedhorn), $a_{12} = 0$ (dot-dashed line corresponding to far field pattern from a pure HE_{11} mode at the aperture), $a_{12} = +0.31$ (solid line corresponding to feed with high Gaussicity), $a_{12} = +0.81$ (dotted line corresponding to feed with high coupling efficiency to an Airy beam). For the high Gaussicity beam horn (solid line) the gain is 20 dB.

1. [Online]. Available: http://www.smtconsultancies.co.uk/.

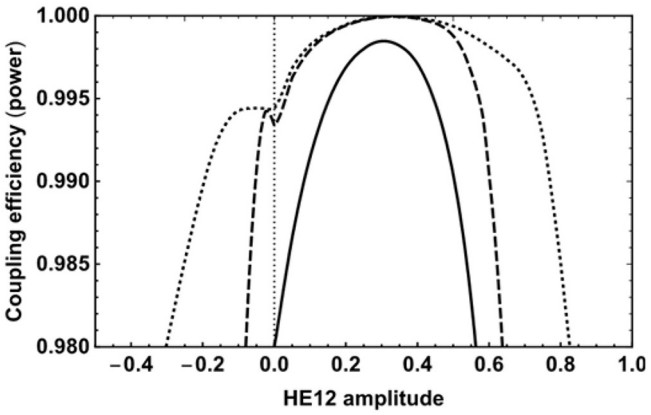

FIGURE 3. Maximal coupling efficiency, as a function of HE_{12} mode amplitude: to a LG_{00} mode (solid line), to a LG_{00} and LG_{02} mode (dashed line), and LG_{00}, LG_{01} and LG_{02} modes (dotted line). It can be seen that for $-0.05 < a_{12} < +0.65$ the output can be approximated as coupling to a fundamental LG_{00} mode with a small LG_{02} content. Outside of that range from $-0.25 < a_{12} < +0.8$, the LG_{01} mode makes a significant contribution.

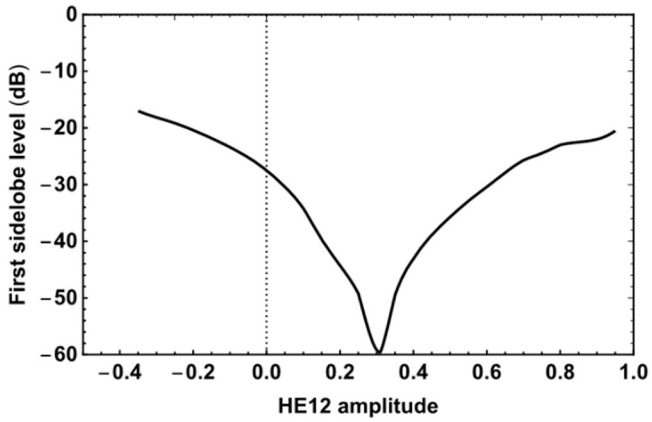

FIGURE 4. First sidelobe level as a function of HE_{12} amplitude assuming no other higher order modes are present and the HE_{11} and HE_{12} modes are in phase at the aperture. The lowest sidelobes are achieved when the Gaussicity is largest at $a_{12} = +0.31$.

r_0 positioned exactly at the aperture, where r_0 is the aperture radius. This creates an output beam with sidelobes at the -28 dB level. This beam will also couple to the LG_{02} mode with 1.6% efficiency. This is not necessarily disadvantageous as the subtle change of beam profile caused by extra LG_{02} Gaussian mode content can lead to improved antenna efficiency with reflection optics, relative to a pure Gaussian beam. Equation (1) shows that in general any gradient within a horn profile will excite higher order modes. Thus, a specific profile is required to excite a pure HE_{11} mode, over extended bandwidths. In Section IV we describe horns of length $\sim 3{r_0}^2/\lambda_c$ with HE_{11} coupling efficiencies above 99.75% across full waveguide bands, where r_0 is the horn aperture radius and λ_c is the center wavelength. It is also possible to use shorter horns with lower coupling efficiency or longer horns which can have coupling efficiencies >99.9% across full waveguide bands. These pure HE_{11} horns form the starting point for most other wideband designs.

B. LAGUERRE GAUSSIAN LG_{00} HORNS

Fig. 3 indicates the coupling efficiency to the LG_{00}, LG_{01} and LG_{02} modes, as a function of HE_{12} amplitude, where it is assumed no higher order HE_{1n} modes are excited. In this graph the chosen Gaussian mode set, at each point, is the one that maximizes power in the LG_{00} mode. It can be seen that the highest coupling to a fundamental LG_{00} Laguerre Gaussian beam (or 'Gaussicity') is achieved at $a_{12} = +0.31$, where 99.87% of power is in the fundamental LG_{00} beam.

It can also be seen that to a very good approximation, for most HE_{12} excitations ($0.05 < a_{12} < 0.6$), corrugated feedhorns primarily couple to just the LG_{00} and LG_{02} beams (>99.5% power coupling, with 99.95% power coupling to just these two modes for $a_{12} = +0.34$). For some applications it can be advantageous to excite both modes, when it is then also important to take the LG_{02} mode into account when calculating beam profiles and specifying the size of optics. It should be noted that for beams containing only even LG_{0n} modes the profile at the aperture will be the same as the far field.

Higher order mode content is a critical determinant of sidelobes, which can be important in many remote sensing and radar applications. Fig. 4 shows the sidelobe levels as a function of HE_{12} amplitude. These can be as low as -60 dB at $a_{12} = +0.31$ for the ideal case, although in practice they can be limited by unwanted low-level excitation of the HE_{13} or higher order modes.

It should be noted that sidelobe levels by themselves are not necessarily good indicators of beam quality. It is entirely possible to construct horns that excite a combination of higher order HE_{1n} and Gaussian modes (not necessarily in phase) that produce apparently low sidelobe levels in the far field, but also yield broad beams. These are rarely optimal for any application.

C. HORNS FOR RADIOMETRY

Radiometers are used to measure accurately the brightness temperature of extended thermal sources and are commonly employed in satellite systems to aid weather forecasting. Such systems often need to operate over extended bandwidths and horn specifications are driven by the need to reduce unwanted extraneous contributions to the measured temperature via sidelobe or spill-over loss. Thus, primary reflectors are often specified with relatively modest edge tapers and far-field beam patterns are primarily determined by the design of the feedhorn. Here, an important characteristic is the fractional power contained in the main beam. This is often specified relative to a multiple of the 3 dB beamwidth. For this application, a pure LG_{00} Gaussian mode is not necessarily the optimum choice. Fig. 5 shows the fractional power within 2.5 times the 3 dB beamwidth as a function of HE_{12} excitation. This has a local maximum around $a_{12} = +0.14$, which is equivalent to adding a small amount of LG_{02} mode in phase with the LG_{00} mode. The main design

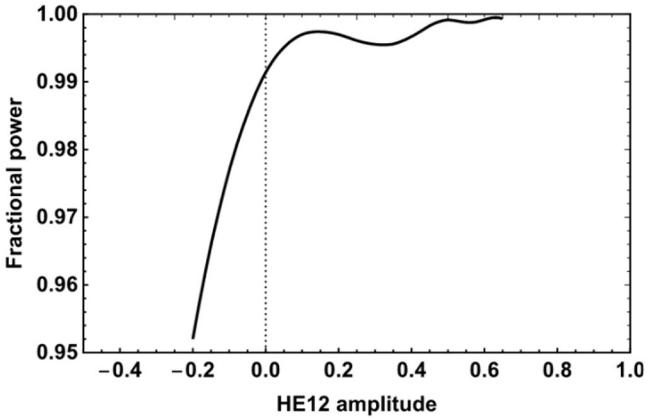

FIGURE 5. Plot showing the fractional power within 2.5 times the 3 dB beamwidth as a function of HE_{12} excitation. It has a local maximum at $a_{12} = +0.14$.

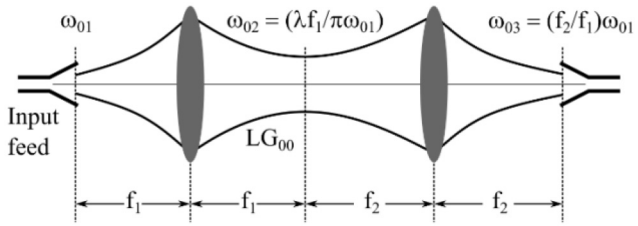

FIGURE 6. Schematic diagram showing the basis of frequency independent optics. An ideal Gaussian telescope will couple perfectly from one fundamental Gaussian beam to another, assuming the effective position of the beam waist, at the horn, remains constant, as a function of frequency. Normally feeds will produce beams with constant beam waists (ω_{01} and ω_{03}) as a function of frequency and have an intermediate focus whose size ω_{02} scales with λ.

challenge is keeping the HE_{11} and HE_{12} modes in phase at the aperture over wide bandwidths. In Section IV we provide illustrative designs where a_{12} can be chosen to approximate $+0.14$ and where the fractional power within 2.5 times the 3 dB beamwidth can exceed 99.5% over a full waveguide band.

It should be noted that the maxima for $a_{12} > +0.40$ correspond to flatter output beams in the far field where the 3 dB points are artificially broad (see Section II-F). Whilst their suitability needs to be evaluated for any given application, this type of excitation can still offer useful solutions where trade-offs are needed between maximizing aperture efficiency, reducing sidelobes and increasing spill-over efficiency.

D. HORNS FOR QUASI-OPTICS

Excitation of a nearly pure Laguerre Gaussian LG_{00} mode is often desirable in generic quasi-optical instrumentation to maximize transmission from feedhorn to feedhorn. In quasi-optical systems using frequency independent optics [18], [19] it is important that the size and position of the beam waist in the horn remains constant as a function of frequency to maintain optimum coupling between horns, as indicated in Fig. 6. In Section III it is shown that for the beam waist to be exactly at the aperture the HE_{12} mode should be kept in phase with the HE_{11} mode at the aperture, across the desired bandwidth.

E. CONSTANT GAIN HORNS

Most LG_{00} feed designs have approximately constant beam sizes at the aperture with respect to wavelength. This means the gain of the horn will vary with frequency, typically by around 4 dB across a waveguide band. Fig. 6 shows the intermediate focus where the beam waist size will now be proportional to the wavelength. It can sometimes be desirable to produce a horn that can couple to this intermediate focus and in effect produce a constant gain horn. Constant gain horns have previously been outlined by Clarricoats *et al.* [2], who pointed out that wide angle linear tapered horns had approximately constant gain for certain taper lengths over limited bandwidths, albeit with rather poor broad beam patterns. A highly compact design with a constant gain operating over 20% bandwidths has also been described for a body scanner application, with low sidelobes and cross-polar < -30 dB and return loss < -22 dB [4]. It can be shown that such a constant gain horn requires precise dispersive properties between modes and in Section IV we demonstrate a design that can operate over full waveguide bands with reasonable beam quality.

F. HORNS TO MAXIMISE APERTURE EFFICIENCY

In a radar, telescope or communications system an important design specification is often the system aperture efficiency over the desired bandwidth. For example, the feedhorns for bands 2 and 3 combined, for the ALMA Cassegrain telescope are specified to provide system aperture efficiencies $>80\%$ at the secondary (also limited by a focusing lens), with sidelobe levels lower than -20 dB and cross-polar better than -25 dB, over 50% bandwidths [10].

For many applications involving a telescope or radar system, the feedhorn should ideally couple with maximum efficiency to the parallel beam received by the primary antenna. A point source in the far field imaged via a circular focusing element will produce an Airy pattern at its focus, as indicated schematically in Fig. 7a. If this Airy-pattern is then imaged using another lens or reflector a "top hat" image of the circular focusing element will form, as indicated schematically in Fig. 7b. The aperture efficiency of an ideal imaging system can be maximized by matching the feed pattern either to the Airy pattern at the first focus (Fig. 7a) or to the top hat pattern at the second focus (Fig. 7b).

The "Airicity" of a beam was a concept introduced by Clarricoats and Poulton [20] and refers to the coupling efficiency at the feedhorn aperture to an Airy pattern given by $(J_1\ (u))/u$, where $J_1(u)$ is the Bessel function of the first kind. In most dish antenna systems, the feeds are designed simply to match to the central lobe of this Airy pattern at their aperture. This limits the maximum possible aperture efficiency to around 84%. A fundamental LG_{00} Gaussian beam matched to this central lobe can provide up to 81.5%

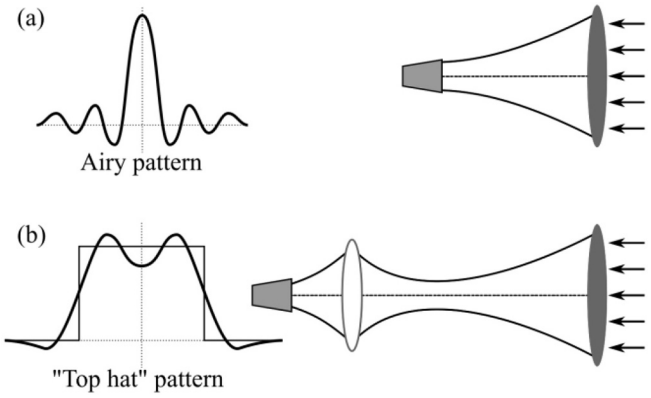

FIGURE 7. (a) The image of a point source in the far field focused through a circular aperture is an Airy pattern. (b) If that image is refocused it will produce a "top hat" pattern. In an ideal system, aperture efficiency can be maximized by matching the input feedhorn pattern to each pattern.

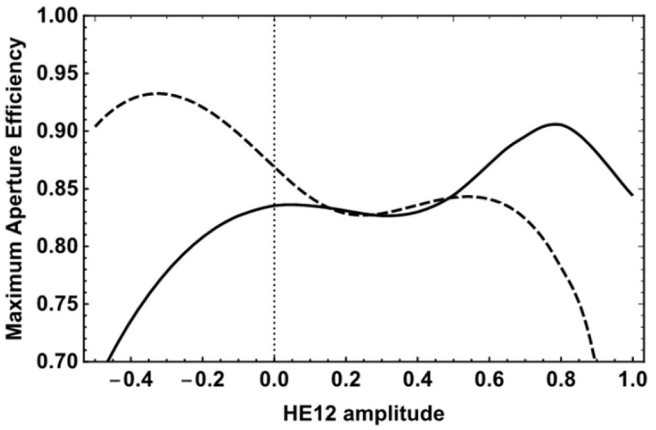

FIGURE 8. Simulated aperture efficiency as a function of HE_{12} amplitude. Solid line shows coupling efficiency to an Airy beam and dashed line shows coupling efficiency to a "top hat" beam.

efficiency. However, it is possible also to match to the next outer lobe in which case the theoretical aperture efficiency can be increased to approximately 91%.

The idea of creating a feed whose output also matches the outer lobes of an Airy pattern is an old one [21], [22], but it had previously been assumed that the bandwidth of such a horn would necessarily be extremely narrow due to the need to excite and precisely phase a number of higher order modes [20]. Such an Airy pattern, at the horn aperture, can be obtained by exciting the HE_{12} mode with an amplitude a_{12} of approximately $+0.81$, and in this paper we show that good efficiencies can be obtained over bandwidths of order 7%. In practical systems, bandwidth may also be partially limited as the width of the main lobe of the Airy pattern also scales with $1/\lambda$.

An alternative to matching to the Airy pattern at the horn aperture is to match to the "top hat" image of the primary produced at the horn aperture, as indicated in Fig. 7b. The optics in the ALMA telescope are designed to achieve this [23]. The width of this pattern will now remain constant as a function of frequency, and the horn will produce an approximation to an Airy beam in the far field. In Section IV-B, we show the design of a horn where $a_{12} \sim -0.15$ ($\theta_{12} = 180°$) over a full waveguide band for which aperture efficiencies at reflector antennas are predicted to be above 90%. Higher efficiencies can be achieved over rather narrower bandwidths by choosing $a_{12} \sim -0.33$ and adding correctly phased higher order modes to match to the higher lobes of the Airy beam in the far field (optics permitting).

Fig. 8 shows the predicted aperture efficiency for these two schemes. The solid line shows theoretical coupling efficiency to an Airy beam at the aperture of the horn and the dotted line shows coupling efficiency to a "top hat" beam. Both schemes offer aperture efficiencies above 90%. However, because of the reduced excitation, the top hat horn can be more compact and operates over larger bandwidths, at the expense of slightly more complicated optics in a telescope.

G. HORNS FOR IMAGING ARRAYS

For some imaging array applications, where a flat response across the aperture is desirable, one can simply maximize the aperture efficiency of individual horns [24]. This is the same as maximizing the coupling efficiency to a "top hat" beam whose width is defined as being equal to the aperture radius of the horn. A corrugated horn with good Gaussian coupling efficiency typically has only 45% aperture efficiency, whereas an HE_{11} horn has almost 70%. The aperture efficiency of an individual horn can increase to more than 80% by adding an HE_{12} component of $a_{12} = -0.40$. To improve on this, further higher order modes must be included at the cost of bandwidth. A design with $a_{12} = -0.37$ and $a_{13} = +0.24$ and $a_{14} = -0.17$ would theoretically provide horn aperture efficiencies above 95%. Simulations show this can be achieved over a narrow bandwidth (few %) and we indicate in Section IV how excitation of these mode-sets can be achieved in practice.

III. HORN CHARACTERISTICS

A. COUPLING TO A GAUSSIAN BEAM

For many corrugated feedhorn applications the object is to maximize coupling to a fundamental LG_{00} Gaussian beam. By taking a coupling integral between the HE_{1n} modes and a fundamental Gaussian mode, it can be shown that the coupling is maximized ($> 99.98\%$) when the HE_{11} and HE_{12} modes are in phase at the aperture and $a_{12} \sim +0.31$. For this case the beam waist ω_0 is approximately $0.50r_0$, where r_0 is the aperture radius, and where we assume no other modes are excited. However, from Fig. 3 it can be seen that Gaussian coupling remains very high ($> 99.9\%$) for a wide range of HE_{12} excitations corresponding to an a_{12} of between $+0.15$ to beyond $+0.40$, giving beam waist radii of between $0.60r_0$ and $0.45r_0$ respectively [14]. In practice, coupling efficiency is limited by excitation of higher order modes.

As noted in Section I, we have previously constructed compact horns with $a_{12} \sim +0.31$ (and $a_{13} \sim +0.03$), which

had very high Gaussicity and −60 dB sidelobes at the center frequency [15]. However, for designs that will operate over a full waveguide band, we show in Section IV (B-C) that it is easier to reduce modal dispersion and unwanted excitation of other modes when $a_{12} \sim +0.15$ to $+0.20$. This leads to beams with narrower central lobes than a pure LG_{00} Gaussian mode, but where the Gaussian coupling efficiency still remains relatively high. (See Section II-C).

B. HORN GAIN AND PHASE CENTER

Because coupling to the fundamental Gaussian mode is so high for a wide range of HE_{12} excitations, it is often useful to be able to work out the gain of the horn and the position of its phase center as a function of the HE_{12} mode content. Kowalski *et al.* [25] has derived analytical expressions that allow the beam radius ω and the radius of curvature R of the dominant fundamental Gaussian beam to be related to the amplitude and relative phase of the HE_{12} mode at the horn aperture:

$$\frac{\omega^2}{{r_0}^2} = 0.436a_{11}^2 + 0.622a_{12}^2 - 0.696a_{11}a_{12}Cos(\theta_{12}) \tag{2}$$

$$\frac{R}{kr_0^2} = \frac{0.436a_{11}^2 + 0.622a_{12}^2 - 0.696\ a_{11}a_{12}\ Cos(\theta_{12})}{4.302a_{11}a_{12}Sin(\theta_{12})} \tag{3}$$

where r_0 is the radius of the aperture of the horn, k is $2\pi/\lambda$, a_{11} and a_{12} are the normalized amplitudes of the HE_{11} and HE_{12} modes and θ_{12} represents the relative phase between the HE_{11} and HE_{12} modes at the aperture. It is also understood that these formulae assume the use of the Gaussian mode set that maximizes the power in the fundamental mode. These quantities can then be easily related to the effective beam waist radius ω_0 of a fundamental Gaussian beam and its position z with respect to the aperture using well known formulae [19]:

$$\omega_0 = \frac{\omega}{\sqrt{1 + \left(\frac{\pi\omega^2}{R\lambda}\right)^2}} \tag{4}$$

$$z = \frac{R}{\left(1 + \left(\frac{R\lambda}{\pi\omega^2}\right)^2\right)}. \tag{5}$$

This analysis was originally applied to excitation of corrugated pipes, but equally applies to corrugated horns. Inspection of these formulae shows that the position of the beam waist (and to a good approximation the phase center) is largely determined by the relative phasing of the HE_{12} mode with respect to the HE_{11} mode. If the HE_{12} mode is in phase at the aperture, the beam waist will be at the aperture and will couple to a fundamental Gaussian beam with a relatively small beam waist and sidelobe levels will be low. If the HE_{12} mode is in antiphase, the beam waist will also be positioned at the aperture. However, it will now couple to a fundamental Gaussian beam with a large beam waist relative to the aperture. This leads to higher sidelobes, but the horn aperture efficiency will be higher. In the general case where the phase θ_{12} is intermediate, the effective beam waist for the fundamental mode will be positioned either behind or in front of the horn aperture and coupling to the fundamental Gaussian mode is reduced.

For many feedhorns, we can use (2) – (5) to identify the Gaussian mode set (given by specifying ω_0 and z) that maximizes coupling to the fundamental Gaussian beam given the amplitude a_{12} and relative phase θ_{12} of the HE_{12} mode. We then use a coupling integral at the aperture to calculate the coupling efficiency to the desired output beam. This will be a good approximation as long as HE_{12} is the only other dominant mode and a_{12} lies between $+0.05$ and $+0.60$. It becomes less exact as ω_0 approaches λ, when higher order modes are required to describe the beam.

If a_{12} remains constant and θ_{12} remains close to 0° (or 180°) then to a good approximation the beam waist size ω_0 and its position will also remain constant as a function of frequency.

C. HORN COMPACTNESS

The total length of the feedhorn is an important specification for many applications. This is particularly true at low microwave frequencies where the length and weight of the horns can easily determine the dimensions of an entire optical sub-assembly, e.g., in a multi-channel radiometer.

Most horns can be scaled for any desired center frequency, and to a reasonable approximation to higher gains (with some caveats related to excitation of higher order modes). The length L of the horn scales with G. λ_c, or equivalently r_0^2/λ_c, where G is the linear horn gain, r_0 is the horn aperture radius, and λ_c is the center wavelength [11]. To allow comparisons of different horn designs we also find it useful to define a dimensionless figure of merit, N_{19dBi}, which is the length L_{19dBi} of a horn with a gain of $8\pi^2$ (19 dBi) measured in wavelengths, at the center wavelength:

$$N_{19dBi} = \frac{L_{19dBi}}{\lambda_c}. \tag{6}$$

A horn with a gain G of $8\pi^2$ is chosen as the reference, since the gain G of a fundamental Gaussian beam is given by $8\pi^2(\omega_0^2/\lambda^2)$ where ω_0 is the effective beam waist radius, [10]. For horns that produce optical outputs that approximate fundamental Gaussian beams, this allows their approximate length L to be conveniently calculated from:

$$L = L_{19dBi}\left(\frac{\omega_0}{\lambda_c}\right)^2 = (N_{19dBi}\lambda_c)\left(\frac{\omega_0}{\lambda_c}\right)^2 \tag{7}$$

where the beam waist ω_0 is chosen to maximize the power in the fundamental mode and measured at the center frequency. It should be noted the ratio ω_0/r_0 will in general be different for each design and is a function of a_{12} and θ_{12} as shown by (2).

In general, most of the wideband horns described here have $N_{19dBi} > 7$ wavelengths, but we note it is possible to design extremely compact feeds with very good performance

over more limited bandwidths. We have previously described a modified tanh-linear design with $N_{19dBi} \sim 3.8$ wavelengths, which has more than 99% coupling efficiency to a fundamental Gaussian beam over 10% bandwidths and −40 dB sidelobe levels at its center frequency [15]. This particular design was recently adapted to provide two highly compact antennas for the quad-band TROPICS cubesat system [17]. In general, there is a trade-off between compactness, bandwidth and performance, particularly at higher gains.

D. RETURN LOSS AND CROSS POLARIZATION

Although this paper is mainly concerned with mode synthesis, the bandwidth of practical feedhorns is also determined by their return loss and cross-polar properties. For the corrugated horns described here, the return loss is largely determined by the matching section at the throat of the horn. The cross-polar component is mainly determined by the level of EH_{11} mode present at the aperture. This is often determined by the throat design, however, the EH_{11} mode can also be excited if the slope of the feed profile becomes too large.

Nevertheless, the design of the matching section at the throat is well understood and has been the subject of several analyses, most notably by Clarricoats *et al.* [2], Dragone [26] and Zhang [27]. For all the horns described, we have adapted the design approach of Zhang. With the exception of the Airy horn (Section IV-F) this throat design leads to simulated return loss and cross-polar excitation better than −30 dB across a full waveguide band (neglecting reflections from the rectangular to circular waveguide transition) as shown in Fig. 9. It is possible to extend the bandwidth to 50% (cross-polar and return loss better than −30 dB) at the cost of a small loss of performance at the center of the band.

IV. EXAMPLE BROADBAND HORNS

In the following section a number of example horn profiles are given that illustrate wideband performance for the applications described in Section II.

Unless otherwise stated, the following horns all have the same quarter wavelength corrugation depth and the same throat designs leading to very similar predicted return loss and cross-polarization properties as illustrated in Fig. 9. All simulations were carried out using the mode-matching program CORRUG. All horns also give highly symmetric patterns with only slight distortions at the band edges. For reasons of clarity, we have chosen to show only the co-polar diagonal (D-plane) antenna pattern, which in almost all cases is a very good approximation to both the E and H patterns for the main lobe.

A. PURE HE_{11} MODE

We have examined a number of profiles to achieve excitation of a pure HE_{11} mode (i.e., $a_{11} = 1$, and $a_{1n} = 0$ for $n > 1$) over large bandwidths in reasonably compact designs. One

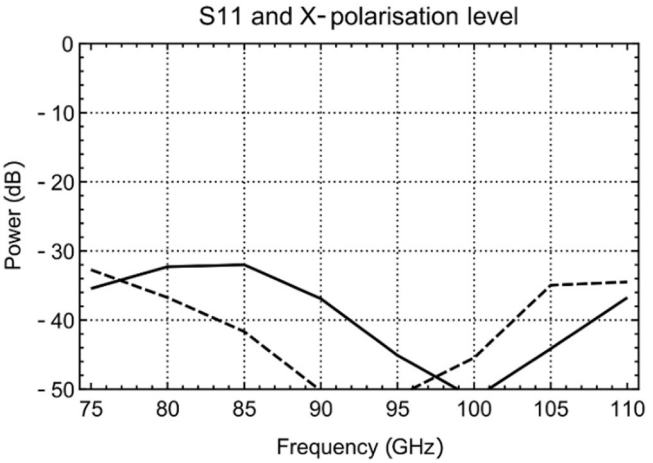

FIGURE 9. Representative return loss (solid line) and cross-polarization (dashed line) as a function of frequency, (both below −30 dB) calculated at 5 GHz intervals for all horns in this work, unless otherwise stated.

practical dual-profile design is to have an initial profile of length L and radius $r(z)$, given by:

$$r(z) = r_i + r_f Sin\left(\frac{\pi z}{2L}\right)^{0.85} \tag{8}$$

where r_i and r_f are the initial and final radii. This is then followed by a second section consisting of a short shallow linear taper that further improves the cancellation of the HE_{12} mode (and other higher order modes). This particular horn does not have a fixed length and in general higher purity HE_{11} modes can be obtained with longer horns, although performance starts to degrade for shorter horns than described here. We obtained this profile through an iterative design optimization process.

The horn has some similarities to a previous design of Granet *et al.* [28], who used a horn with a $Sin(\pi z/2L)^{0.8}$ profile as a feed for Earth observation studies, and to the corrugated Winston Cone described by Maffei *et al.* [29], although neither was designed with pure HE_{11} mode excitation in mind.

An example of a 25 dBi HE_{11} mode horn is shown in Fig. 10a, with a center frequency of 94 GHz, where the bowl-like profile is 80 mm long, the shallow linear taper is 35 mm long and the horn aperture is 22 mm diameter. The length L of this horn is $L \sim 3r_0^2/\lambda_c$, which corresponds to $N_{19dBi} = 7.3$ wavelengths

Fig. 10b shows the far field beam pattern, with sidelobes around −28 dB (as expected for a pure HE_{11} mode) and beamwidths consistent with a constant beam waist at the aperture, independent of frequency. The illustrative design shown here provides > 99.9% power coupling efficiency to the HE_{11} mode at the center of the band and > 99.75% power coupling efficiency to the HE_{11} mode over a 50% bandwidth with the HE_{12} mode largely making up the residual ($|a_{12}| < 0.04$). It is also possible to increase coupling efficiency further by using the same generic design but lengthening the horn.

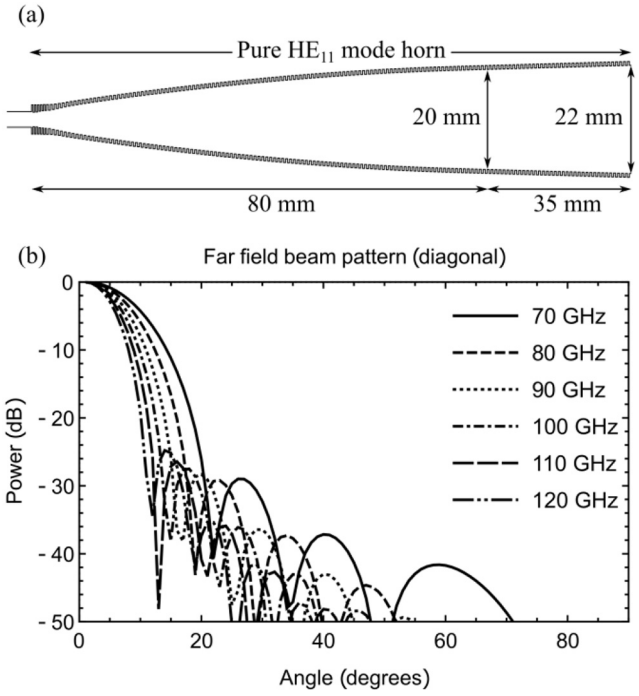

FIGURE 10. (a) Example HE_{11} horn profile and (b) resulting far-field beam pattern. A pure HE_{11} mode will produce beams with sidelobes at −28 dB.

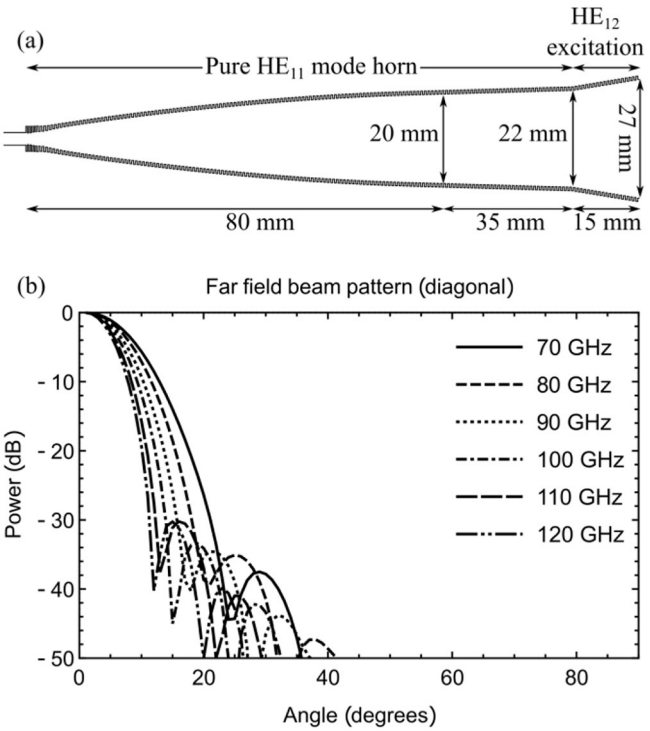

FIGURE 11. (a) Illustrative profile of a very wideband ∼25 dBi Gaussian horn consisting of a HE_{11} mode horn followed by a short taper to excite the HE_{12} mode. (b) The resulting far-field pattern. The horn has excellent wideband performance. The sidelobe level is mainly due to unwanted excitation of the HE_{13} mode.

B. GAUSSIAN EXCITATION VIA A SHORT LINEAR TAPER

It is then possible to improve the Gaussicity of the output beam by adding another steeper linear taper to the pure HE_{11} horn to deliberately excite the HE_{12} mode, as shown in Fig. 11a. The length of this taper should be small compared to the relevant phasing wavelength $\lambda_{1n}(r) = (1/\lambda_{HE11}(r) - 1/\lambda_{HE1n}(r))^{-1}$. In this case, the HE_{12} excitation will be almost constant with frequency, and there will be a small constant phase difference between the modes, leading to a fixed phase center. There is a trade-off regarding the length and slope of this taper. If the taper is too long then there is too much dephasing of the HE_{12} mode, introducing beam distortions (over extended bandwidths). However, if it is too short there will either be too little HE_{12} excitation, or if too steep, too much excitation of the HE_{13} and EH_{11} modes, which, respectively, increases sidelobe content and cross-polar content. Typically choosing a value of a_{12} between +0.12 and +0.20 and a phase difference θ_{12} not much more than 35° leads to a beam waist with an approximately constant phase center positioned behind the aperture. This provides relatively high quality beam patterns over 50% bandwidths as shown in Fig. 11b.

Sidelobes are between −30 dB and −37 dB and are limited largely by unwanted excitation of the HE_{13} mode that becomes more significant at higher frequencies. This type of horn is particularly suitable for wideband coupling between two feedhorns in quasi-optical systems. This design appears similar to a wideband horn recently developed using numerical optimization techniques [30] and is of the same design family as the horns used for the Planck HFI telescope [8].

For the particular design shown, $N_{19dBi} \sim 7.8$ wavelengths, or $L \sim 2.25r_0^2/\lambda_c$ where r_0 is the aperture radius. Note that the expression for L appears smaller than for the previous pure HE_{11} horn design, because the aperture radius r_0 is larger (for comparable gain).

Numerous papers have also suggested using a Gaussian flare that mimics the shape of the Gaussian beam (following excitation of a mode that approximates an HE_{11} mode). The general claim is that high purity Gaussian beams are naturally produced, as long as the flare is a reasonable fraction of a Raleigh range. Whilst this can be true over a range of frequencies, especially at lower gains [9], at this aperture we did not find this scheme worked as well over extended bandwidths, compared to the approaches outlined above, and in the next section.

C. GAUSSIAN BEAM WITH HALF SINUSOID PROFILE

In the previous short linear taper design, there will always be a constant phase shift between the two main modes. As an alternative that produces higher quality beams over a marginally reduced bandwidth, it is also possible to add a half sinusoidal section with a radial profile $r(z)$ given by:

$$r(z) = r_0 + A_2 Sin\left(\frac{2\pi z}{\lambda_{12}(r)} + \phi_2\right) - A_2 Sin(\phi_2) \qquad (9)$$

where A_2 is the radial modulation amplitude and ϕ_2 represents the starting phase of the radial modulation for the HE_{12} mode. The phasing wavelength $\lambda_{12}(r) =$

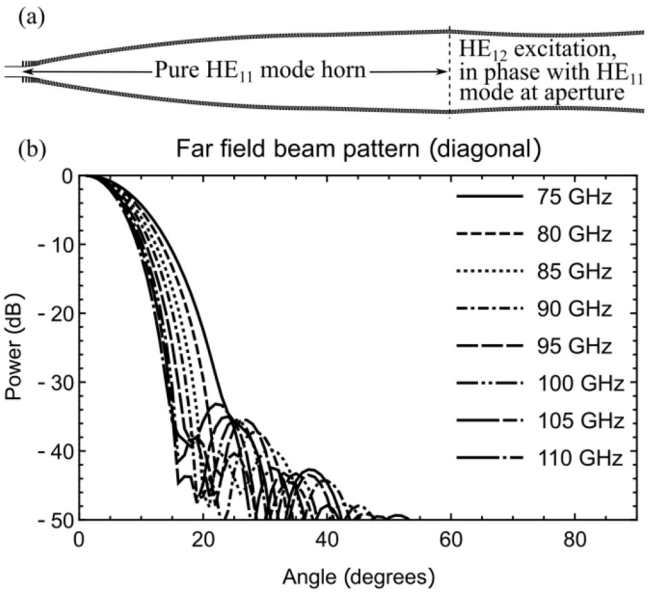

FIGURE 12. (a) HE_{11} horn with a following sinusoidal section. This horn has low dispersion with the phase center now being positioned at the horn aperture across the band. (b) The resulting far-field pattern. Sidelobes are lower compared to the horn in Fig. 11 due to lower HE_{13} excitation.

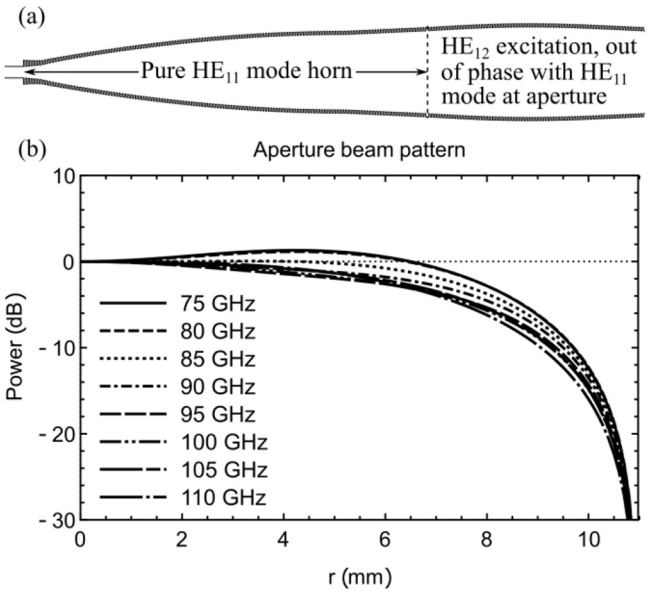

FIGURE 13. (a) HE_{11} horn followed by sinusoidal section designed to excite, with low dispersion (b) a "top hat" beam at the horn aperture. This aperture pattern will excite an Airy beam in the far field.

$(1/\lambda_{HE11}(r) - 1/\lambda_{HE12}(r))^{-1}$ is specified at the low frequency end of the band to reduce dispersion and maximize bandwidth. This sinusoidal modulation means the excited HE_{12} mode will interfere constructively with the propagating HE_{12} mode, in a manner analogous to quasi-phase matching in optical parametric oscillators. It thus provides selective enhancement of that mode, whereas other modes will tend to interfere destructively. The large advantage, at least for moderate excitations ($|a_{12}| \sim 0.12 - 0.20$), is that modal dispersion can be almost eliminated over a full waveguide band, whilst excitation of the HE_{13} mode is reduced relative to the short linear taper design shown in Fig. 11. With optimization, the HE_{12} mode can now remain in phase with the HE_{11} mode, at the aperture, to within $\pm 10°$ over 40% bandwidths. This can be contrasted with the $\sin^2$-parallel and tanh-linear designs where phase slippage typically reaches $\pm 115°$ over a full waveguide band, limiting effective bandwidths to around 20%.

An example of a horn with $\phi_2 = 180°$ is shown schematically in Fig. 12a. This horn deliberately excites the LG_{02} mode in phase with the LG_{00} mode at the aperture to produce a narrow beam with >99.5% of its power within 2.5 of the 3 dB angular beamwidth across the band. The phase center is also positioned at the aperture and is essentially constant with frequency varying by no more than ± 0.05 of a Raleigh range. Sidelobes at the center of the band are below -40 dB. It has a similar length L, for similar gain, compared to the $\sin^2$-parallel design [13], but works over significantly wider bandwidths. In this example, $L \sim 3r_0^2/\lambda_c + 1.6r_0^2/\lambda_L$ where λ_c is the center wavelength and λ_L is the wavelength at the low frequency end of the band. This corresponds to $N_{19dBi} \sim 15.5$ wavelengths. Far-field patterns across a waveguide band are shown in Fig. 12b.

This type of horn is suited both for wideband quasi-optics, and radiometric (and radar) applications, where high-quality narrow beams with constant phase centers are important.

D. "TOP HAT" BEAM WITH HALF SINUSOID PROFILE

A variation of the previous horn design where now $\phi_2 = 0°$, is shown in Fig 13a. This design puts the HE_{12} mode almost exactly 180° out of phase with the HE_{11} mode and now produces an approximation to a "top hat" profile at the aperture, (and an Airy-pattern in the far-field), across a full waveguide band, as indicated in Fig. 13b. The length of this horn, compared to the previous example, can also be calculated from $L \sim 3r_0^2/\lambda_c + 1.6r_0^2/\lambda_L$ but N_{19dBi}, now approximates 9.4 wavelengths, due to the higher horn aperture efficiency.

This type of horn has a horn aperture efficiency of 75% and can couple to a "top hat" beam with ~90% efficiency, both across a full waveguide band. This efficiency can be improved by exciting higher order modes as further discussed in Section IV-G.

E. GAUSSIAN HORNS WITH MULTIPLE SINUSOIDS

In general, for a single half sinusoid there is a limit to the radial modulation amplitude A_2 before excitation of higher order modes (HE_{13} and EH_{11}) limits performance. Thus, for larger excitations (e.g., $a_{12} > +0.2$) or more complex excitations, more radial oscillations are required, and the horn becomes longer and bandwidth decreases. This bandwidth can nevertheless be substantially greater than methods that excite the higher order mode(s) near the throat of the horn. They are also easier to scale for any desired gain.

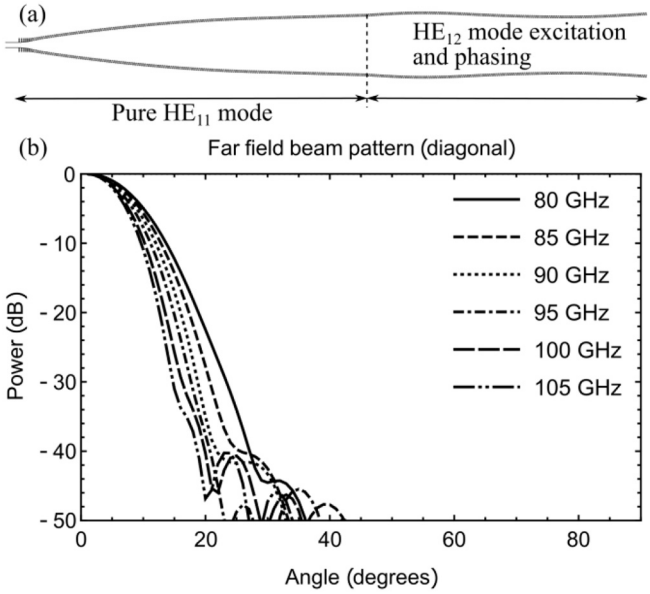

FIGURE 14. (a) HE_{11} mode horn with double sinusoidal section and (b) resulting far field beam pattern. This horn reduces unwanted HE_{13} excitation further reducing sidelobes but with slightly reduced bandwidth.

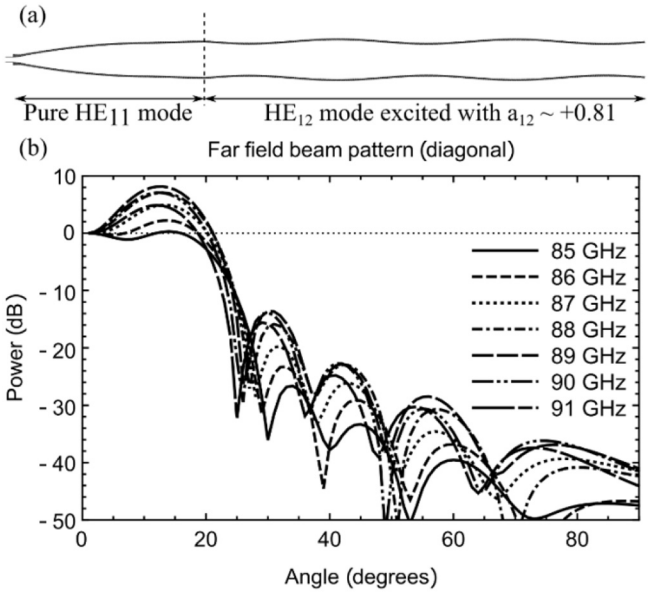

FIGURE 15. (a) HE_{11} horn followed by multiple sinusoidal section to excite a HE_{12} mode with $a_{12} \sim +0.81$. This creates an Airy mode at the aperture, which (b) excites a "top hat" type mode in the far field.

Thus, Fig. 14a shows a pure HE_{11} feed with two additional sinusoidal half-cycles whose length $L \sim 3r_0^2/\lambda_c + 3.2r_0^2/\lambda_L$. This has the effect of allowing increased a_{12} amplitude, whilst reducing HE_{13} amplitude. Fig. 14b shows this leads to horns with lower sidelobes (< -40 dB), at the cost of slightly reduced bandwidth. Bandwidth now starts to be limited by modal dispersion, as can be seen by the slight distortion (shoulder) seen at the very low end of the band where $|\theta_{12}| > 35°$.

F. AIRY BEAM HORN

As another example of a horn that uses multiple sinusoidal cycles, Fig. 15a shows a horn that produces an Airy-pattern at its aperture. The resulting "top hat" far-field beam patterns are shown in Fig. 15b. The horn is comprised of a pure HE_{11} horn to which 5 sinusoidal half-cycles have been added. This horn now becomes relatively long ($L \sim 3r_0^2/\lambda_c + 8r_0^2/\lambda_L$) as several modulation periods are needed to excite the required amplitude $a_{12} \sim +0.81$, without excessively exciting the HE_{13} or EH_{11} modes. This horn can allow aperture efficiencies $> 90\%$ to be obtained over $\sim 7\%$ bandwidths, limited by modal dispersion. For this specific horn, the cross-polar level is degraded with respect to the performance shown in Fig. 9, with levels more in the range of -20 dB to -30 dB.

G. COMPLEX MODE EXCITATIONS

Synthesis of more complex output beams requires excitation and phasing of multiple higher order Gaussian beams, requiring excitation and phasing of multiple HE_{1n} modes.

In general, at a given frequency, this can be achieved by sinusoidally modulating the horn radius $r(z)$ over a length z at a number of different radial frequencies, with different radial amplitudes A_n and different starting phases ϕ_n according to the desired excitation. The profile is then given by:

$$r(z) = r_0 + \Sigma\left\{A_n Sin\left(\frac{2\pi z}{\lambda_{1n}(r_0)} + \phi_n\right) - A_n Sin(\phi_n)\right\} \quad (10)$$

where the phasing wavelength $\lambda_{1n}(r)$ at radius r is given by:

$$\lambda_{1n}(r) = \left(\frac{1}{\lambda_{HE11}(r)} - \frac{1}{\lambda_{HE1n}(r)}\right)^{-1} \quad (11)$$

where $\lambda_{HE1n}(r)$ is the wavelength of the HE_{1n} mode at radius r, A_n is the radial modulation amplitude, ϕ_n is a starting phase (often 0° or 180° for HE_{12}) and the summation is just over the first few HE_{1n} modes. In practice, optimization algorithms need to be run as the mode excitations are not completely independent. However, optimization is now relatively quick due to the limited number of input variables. Bandwidth decreases as higher order modes are added.

For example, it is possible to increase the "top hat" and horn aperture efficiency of the feedhorn by adding higher order modes within the horn, to create a better approximation to a "top hat" excitation at the aperture e.g., $a_{12} = -0.37$, $a_{13} = +0.23$, $a_{14} = -0.17$.

Figure 16a shows a design where the first two modes are excited using (10), and Fig. 16b shows the resulting aperture pattern. This horn couples to a "top hat" beam with efficiencies of 88% across the band with 95% at band center and has a horn aperture efficiency of 80% across a waveguide band with 87% at band center.

H. CONSTANT GAIN FEEDHORNS

In all the horns described above, the effective beam waist ω_0 stays roughly constant, and so horn gain G will vary with frequency, typically by 4 dB over a waveguide band.

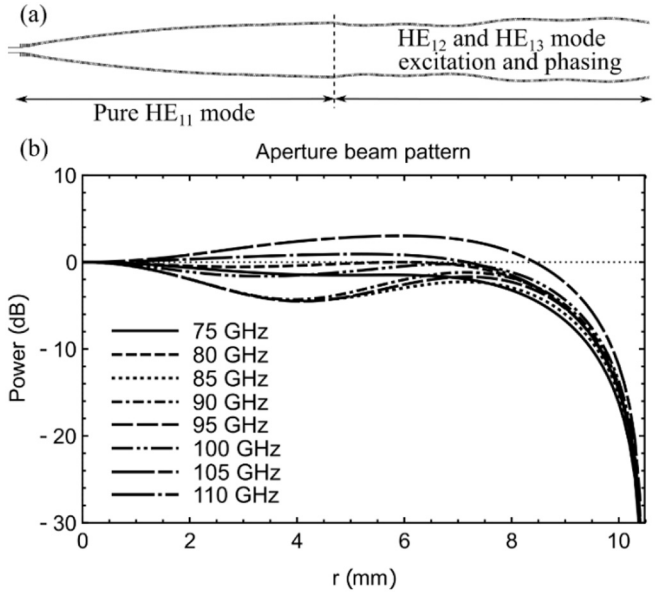

FIGURE 16. (a) HE_{11} horn followed by complex profile to optimally excite HE_{12} and HE_{13} modes to create (b) an improved "top hat" beam at the aperture. This should be compared to Figure 13.

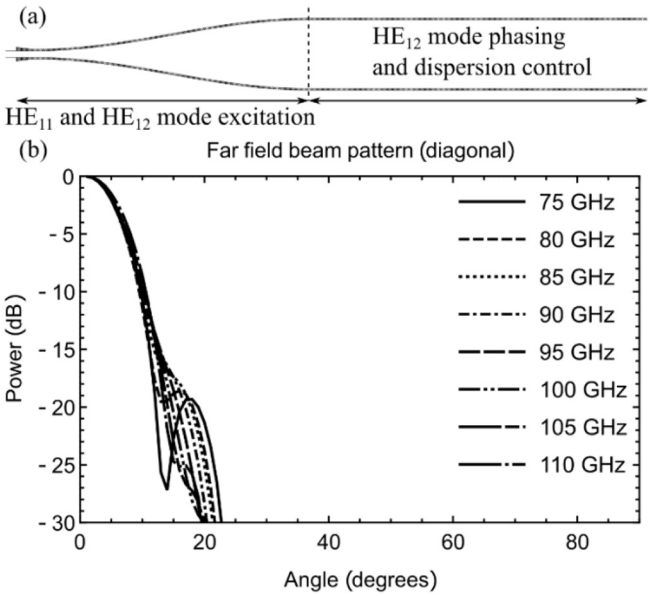

FIGURE 17. (a) A $\sin^2$-parallel horn designed to have the required dispersion to create a constant gain horn. (b) The resulting far field beam pattern.

This can be seen from the expression for gain G of a fundamental Gaussian beam, $G = 8\pi^2(\omega_0^2/\lambda^2)$. However, it is also possible to design feedhorns with constant gain, where ω_0 must now be made to scale with λ. Inspection of (2) – (5) shows that this requires the feedhorn to be strongly dispersive (both a_{12} and θ_{12} varying with frequency).

One wideband solution is to utilize the modal phase dispersion naturally present in the $\sin^2$-parallel horn [13]. It is found for full band horns that the necessary dispersion can be achieved if the length of the initial section is chosen to excite a HE_{12} mode amplitude $a_{12} = +0.35$ at the center frequency. The phasing length is then chosen so that the HE_{12} mode is in phase with the HE_{11} mode at the highest frequency over the desired bandwidth. In other words, the phase center is positioned at the aperture at the highest frequency and its position moves further inside the horn as frequency is lowered. In general, there is a trade-off between beam quality and required bandwidth, and sidelobe performance can be improved considerably over narrower bandwidths.

This design is illustrated schematically above in Fig. 17a. Fig. 17b shows a plot of simulated far-field antenna patterns at 5 GHz intervals over a full waveguide band (75-110 GHz). Beam patterns are effectively constant out to a 15 dB edge taper. The phase center now moves over ± 0.2 of a Raleigh range $z_R = \pi\omega_0^2/\lambda_c$, which can be acceptable, but the effect on phase efficiency would need to be checked for a given design requirement. The example presented is for a horn with a center frequency of 94 GHz and a gain of 25.5 dBi. This corresponds to a horn $L \sim 4.3r_0^2/\lambda_c$ or $N_{19dBi} \sim 17.3$ wavelengths. This horn is illustrative of one design approach. Much higher performance is possible at reduced bandwidths.

V. DISCUSSION AND SUMMARY

We have shown that many wideband high-performance feed designs can simply depend on the correct excitation (a_{12}) and relative phasing (θ_{12}) of the HE_{12} mode. A simple conical corrugated horn can have acceptable performance, especially compared to a smooth horn, but is rarely optimal as it excites the HE_{12} mode (where a_{12} is length dependent from (2)) approximately 90° out of phase with the HE_{11} mode.

An alternative approach (at least for horns designed to excite a Gaussian LG_{00} beam) is the generic Gaussian flared horn approach [9], [31]. These designs can provide good beam patterns in rather compact horns, over reasonable bandwidths, especially at low gains [9]. This style of horn usually has a beam waist whose position is both a function of frequency and relatively far inside the horn which will lead to a complex mode distribution at the aperture. This makes them less amenable to more complex mode synthesis, at least over extended bandwidths.

In this paper, we have indicated optimal excitations for different applications, and have shown how low dispersion structures can lead to wideband performance, relative to other published wideband designs [9], [31], [32]. Many of the designs described have near constant phase centers and produce optical beams with very similar mode content and modal phasing across their specified bandwidth. The different designs discussed in this paper are summarized in Table 1, along with other lower bandwidth "dispersive" horns also mentioned in this paper. Table 1 gives sidelobe level (SL) at the center frequency, approximate (conservative) percentage bandwidth (BW), and two measures of relative compactness for different designs.

The HE_{11} horn (Fig. 10), with $a_{12} \sim 0$, provides excellent coupling to a corrugated pipe transmission line.

TABLE 1. Table indicating some of the key characteristics of the horns illustrated in this paper. *SL* is the sidelobe level in dB at the center frequency. *BW* gives an indication of the approximate percentage bandwidth. a_{12} and θ_{12} give the target excitations of the HE_{12} mode where applicable. N_{19dBi} is the effective length of a 19 dBi horn at the center wavelength and *length* gives the approximate length of the horn in units of r_0^2/λ_c where r_0 is the aperture radius and λ_c is the center wavelength.

Horn Type (advantage)	**SL** (dB)	**BW** (%)	a_{12} at λ_c	θ_{12} (deg)	N_{19dBi} (λ_c)	**Length** (r_0^2/λ_c)
Conical (simple)	-28	var	var	~ 90	var	var
Sin^2-parallel [15] (Easy to design)	-37	20	0.2	± 35	15.5	4.4
Tanh-Lin1 [15] (very compact)	-40	20	0.2	± 35	3.8	0.94
Tanh-Lin2 [15] (high Gaussicity)	-60	20	0.31	± 35	12.4	3.0
Low Dispersion Feeds (this paper)						
HE_{11} (Fig. 10) coupling to corrugated pipe	-28	50	0	NA	7.3	3.0
HE_{11} + Flare (Fig. 11) opt. 2.5 x 3dB	-34	50	0.15	30	7.8	2.25
HE_{11} + 1/2 x Sine (Fig. 12) opt. 2.5 x 3dB	-37	40	0.15	0	15.5	4.3
HE_{11} + 2 x Sine (Fig. 13) high Gaussicity	-50	30	0.25	0	20.8	6
HE_{11} + 5 x Sine (Fig. 15) Airy Horn	NA	7	0.81	0	NA	9.6
HE_{11} – 1/2 x Sine (Fig 14) Top Hat Horn	-22	40	0.2	180	9.4	4.8
Max App Eff. (Fig 16) Horn array	-18	10	0.37	180	10.6	6.5
Constant Gain (Fig. 17)	-18	40	var	var	17.3	4.3

For radiometry, $a_{12} \sim +0.14$ (with $\theta_{12} = 0$) excites a LG_{00} and LG_{02} combination that provides relatively low sidelobes and narrow beams that maximizes power within 2.5 of the 3 dB beam angle. This can be achieved by a simple taper (Fig. 11) or a single half-sinusoid with slightly better performance (Fig. 12). These types of horns are also suitable for wideband quasi-optical instrumentation.

Gaussicity (pure LG_{00} excitation) improves as a_{12} increases further, which can be achieved by adding extra half sinusoids at the cost of a slight reduction in bandwidth (Fig. 13, with $a_{12} \sim +0.25$). For $a_{12} > +0.32$ the beam starts to distort, and at $a_{12} \sim +0.81$ the beam resembles an Airy pattern at the aperture (Fig. 15).

High system aperture efficiency is typically desired for radar and communication systems, and both "Airy" and "top hat" design horns can, in principle, be used to improve system aperture efficiency to around 90% with ideal dish antennas. "Top hat" designs are more compact and operate over wider bandwidths than "Airy" designs, but require an additional focusing element if used in a telescope (see Fig. 7b).

"Top hat" beam patterns at the aperture can be obtained by making $\theta_{12} = 180°$ and Fig. 14 illustrates a wideband design where $a_{12} = -0.2$. Higher coupling efficiency to "top hat" beams is also desirable for horn arrays and can be further improved by exciting and phasing other higher order modes. Fig. 16 shows a design where $a_{12} \sim -0.37$, and $a_{13} \sim -0.2$, where 80% horn aperture efficiencies across a full waveguide band can be achieved, with higher efficiencies at the center frequency.

Finally, Fig. 17 shows a design that is deliberately dispersive to provide a feedhorn that has constant gain over a full waveguide band.

All feedhorns described in this paper can be scaled both for center frequency and for gain, although, it should be noted that better performance can be expected for smaller apertures (and lower gain) where higher order modes can be below or near to cut-off. Simulations also show it is possible to further improve performance for a given design if the total bandwidth is reduced, even moderately.

We do not claim to have fully explored the parameter space, or fully optimized the horns given, and there is always scope to trade-off different performance parameters within a given design, particularly when highly compact horns are required. However, we believe these designs give new starting points, which allow efficient optimization algorithms to be run, with a restricted set of input parameters for a given target specification. They also give system designers an indication of what can be realistically achieved for a given target mode excitation. In many cases we believe the wideband characteristics of many of these feeds already represent state-of-the-art performance.

ACKNOWLEDGMENT

The authors would like to acknowledge useful discussions with Dr. Soe Min Tun, author of the CORRUG program, and to acknowledge the previous work of Dr. Johannes McKay whilst he was at the University of St Andrews. Nina Thomsen currently works at SINTEF Energy Research, Trondheim Norway. Stuart Macpherson currently works at the Cavendish Laboratory, University of Cambridge, U.K. Dr. Richard Wylde is Managing Director of Thomas Keating Ltd., Billingshurst, U.K. and is an honorary member of staff in the School of Physics and Astronomy, University of St Andrews, U.K.

REFERENCES

[1] P. J. B. Clarricoats and A. D. Olver, *Corrugated Horns for Microwave Antennas*. London, U.K.: Inst. Eng. Technol., 1984.
[2] P. J. B. Clarricoats, A. D. Olver, A. A. Kisk, and I. Shafei, *Microwave Horns and Feeds*. London, U.K.: Inst. Eng. Technol., 1994.
[3] C. Granet and G. L. James, "Design of corrugated horns: A primer," *IEEE Antennas Propag. Mag.*, vol. 47, no. 2, pp. 76–84, Apr. 2005.
[4] J. Teniente, J. C. Iriarte, I. Ederra, and R. Gonzalo, "Advanced feeds for mm-wave antenna systems," in *Aperture Antennas for Millimeter and Sub-Millimeter Wave Applications*, A. Boriskin and R. Sauleau, Eds. Cham, Switzerland: Springer, 2018.
[5] J. Pressensé, P. E. Frandsen, M. Lumholt, F. Delepaux, A. Frandsen, and L. S. Drioli, "Optimizing a corrugated horn for telecommunication and tracking missions using a new flexible horn design software," in *Proc. 4th Eur. Conf. Antennas Propag.*, 2010, pp. 1–5.

[6] J. Teniente, R. Gonzalo, and C. Del-Rio, "Ultra-wide band corrugated Gaussian profiled horn antenna design," *IEEE Microw. Wireless Compon. Lett.*, vol. 12, no. 1, pp. 20–21, Jan. 2002.
[7] F. Villa *et al.*, "Planck LFI flight model feed horns," *J. Instrum.*, vol. 4, Jan. 2010, Art. no. T12004.
[8] B. Maffei *et al.*, "Planck-HFI optical design and pre-fight performances," in *Proc. 4th Eur. Conf. Antennas Propag.*, 2010, pp. 1–5.
[9] J. Teniente-Vallinas, R. Gonzalo-Garcia, and C. Del-Rio-Bocio, "Modern Corrugated Horn Antenna Design for extremely low sidelobe level," presented at the 26th ESA Antenna Technol. Workshop Satellite Antenna Model. Des. Tools, 2003.
[10] A. Gonzalez, "ALMA band 2+3 (67–116 GHz) optics: Design and first measurements," presented at the IEEE Int. Symp. Antennas Propag. (APSURSI), Fajardo, Peurto Rico, 2016.
[11] J. Doane, "Propagation and mode coupling in coorugated and smooth-wall circular waveguides," in *Millimeter Components and Techniques*, K. J. Button, Ed. Orlando, FL, USA: Academic, 1985, pp. 123–170.
[12] A. D. Olver and J. Xiang, "Design of profiled corrugated horns," *IEEE Trans. Antennas Propag.*, vol. 36, no. 7, pp. 936–940, Jul. 1988.
[13] P. A. S. Cruickshank, D. R. Bolton, D. A. Robertson, R. J. Wylde, and G. M. Smith, "Reducing standing waves in quasi-optical systems by optimal feedhorn design," presented at the Joint 32nd Conf. Infrared MM-Waves 15th Conf. THz Electron., Cardiff, U.K., 2007.
[14] J. E. McKay *et al.*, "Compact wideband corrugated feedhorns with ultra-low sidelobes for very high performance antennas and quasi-optical systems," *IEEE Trans. Antennas Propag.*, vol. 61, no. 4, pp. 1714–1721, Apr. 2013.
[15] J. E. McKay, D. A. Robertson, P. J. Speirs, R. I. Hunter, R. J. Wylde, and G. M. Smith, "Compact corrugated feedhorns with high Gaussian coupling efficiency and –60 dB sidelobes," *IEEE Trans. Antennas Propag.*, vol. 64, no. 6, pp. 2518–2522, Jun. 2016.
[16] A. Murk, N. Kämpfer, R. J. Wylde, J. Inatani, T. Manabe, and M. Seta, "Characterization of various quasi-optical components for the submillimeter limb-sounder SMILES," in *Proc. 12th Int. Symp. Space THz Technol.*, San Diego, CA, USA, 2001, pp. 426–435.
[17] I. Osaretin, W. Blackwell, R. Wylde, S. M. Tun, and G. M. Smith, "High-performance reflector antenna design for the TROPICS mission," in *Proc. IEEE Int. Symp. Antennas Propag. USNC/URSI Nat. Radio Sci. Meeting*, 2018, pp. 1719–1720.
[18] A. Gonzalez, "Frequency independent design of quasi-optical systems," *J. Infrared Millim. Waves THz*, vol. 37, pp. 147–159, Feb. 2016.
[19] P. F. Goldsmith, *Quasioptical Systems*. New York, NY, USA: IEEE Press, 1998.
[20] P. J. B. Clarricoats and G. T. Poulton, "High-efficiency microwave reflector antennas—A review," *Proc. IEEE*, vol. 65, no. 10, pp. 1470–1503, Oct. 1977.
[21] A. C. Ludwig, "Radiation pattern synthesis for circular aperture horn antennas," *IEEE Trans. Antennas Propag.*, vol. TAP-14, no. 4, pp. 434–440, Jul. 1966.
[22] R. Padman, J. A. Murphy, and R. E. Hills, "Gaussian mode analysis of Cassegrain antenna efficiency," *IEEE Trans. Antennas Propag.*, vol. TAP-35, no. 10, pp. 1093–1103, Oct. 1987.
[23] J. W. Lamb, "Low-noise, high-efficiency optics design for ALMA receivers," *IEEE Trans. Antennas Propag.*, vol. 51, no. 8, pp. 2035–2047, Aug. 2003.
[24] A. K. Bhattacharyya and G. Goyette, "A novel horn radiator with high aperture efficiency and low cross-polarization and applications in arrays and multibeam reflector antennas," *IEEE Trans. Antennas Propag.*, vol. 52, no. 11, pp. 2850–2859, Nov. 2004.
[25] E. J. Kowalski, M. A. Shapiro, and R. J. Temkin, "Simple correctors for elimination of high-order modes in corrugated waveguide transmission lines," *IEEE Trans Plasma Sci*, vol. 42, no. 1, pp. 29–37, Jan. 2014.
[26] C. Dragone, "Characteristics of a broadband microwave corrugated feed: A comparison between theory and experiment," *Bell Syst. Tech. J.*, vol. 56, no. 6, pp. 869–888, Jul./Aug. 1977.
[27] X. Zhang, "Design of conical corrugated feed horns for wide-band high-frequency applications," *IEEE Trans. Microw. Theory Techn.*, vol. 41, no. 8, pp. 1263–1274, Aug. 1993.
[28] C. Granet, T. S. Bird, and G. L. James, "Compact multimode horn with low sidelobes for global earth coverage," *IEEE Trans. Antennas Propag.*, vol. 48, no. 7, pp. 1125–1133, Jul. 2000.
[29] B. Maffei, E. Gleeson, J. A. Murphy, and G. Pisano, "Study of corrugated Winston horns," in *Proc. SPIE*, vol. 5498, 2004, pp. 812–817.
[30] L. Zeng, C. E. Tong, E. J. Wollack, and D. T. Chuss, "A wideband profiled corrugated horn for multichroic applications," presented at the 40th Int. Conf. Infrared Millimeter THz Waves (IRMMW-THz), Hong Kong, 2015.
[31] J. Teniente, R. Gonzalo, and C. Del-Rio-Bocio, "Ultra-wideband corrugated Gaussian profiled horn antenna design," presented at the IEEE Microw. Wireless Compon. Lett., 2001.
[32] C. Del-Rio, R. Gonzalo, and M. Sorolla, "High purity Gaussian beam excitation by optimal horn antenna," in *Proc. Int. Symp. Antennas Propag.*, Chiba, Japan, 1996, pp. 1133–1136.